Effect of Fly Ash and PVA Fiber on Microstructural Damage and Residual Properties of Engineered Cementitious Composites Exposed to High Temperatures

Mustafa Şahmaran[1]; Erdoğan Özbay[2]; Hasan E. Yücel[3]; Mohamed Lachemi[4]; and Victor C. Li[5]

Abstract: This paper discusses the influence of high volumes of fly ash and micro polyvinyl alcohol (PVA) fibers on the fire resistance and microstructure of engineered cementitious composites (ECC). Composites containing two different contents of fly ash as a replacement for cement (55 and 70% by weight of total cementitious materials) are examined. To determine the effects of microfibers and ultrahigh ductility of ECC, ECC matrix mixtures of similar composition except PVA fiber are also produced and tested for the fire resistance. The mixtures are exposed to temperatures up to 800°C for one hour. Fire resistances of the mixtures are then quantified in terms of the residual mechanical properties (strength, stress-strain curve, deflection, and stiffness) and mass loss. The role of PVA fibers and fly ash is discussed through the analysis of microstructure and fiber-matrix interactions as a function of heat treatment. The microstructural characterization is examined before and after exposure to fire deterioration by using scanning electron microscopy and the pore size distribution is obtained by mercury intrusion porosimetry. Results indicate that adding micro PVA fiber to the ECC matrix substantially improves the fire resistance and eliminates the explosive spalling behaviors of the ECC matrix. Fire resistance of ECC mixtures is further improved with the increase of fly ash content. **DOI: 10.1061/(ASCE)MT.1943-5533.0000335.**

CE Database subject headings: Composite materials; Fly ash; Fires; Microstructures; Temperature effects.

Author keywords: Engineered cementitious composites; Fire resistance; Fly ash; PVA fibers; Microstructure.

Introduction

Concrete is the most widely used construction material in the world. Although it was primarily designed for carrying compressive loads, concrete in real field conditions is also subjected to tensile stresses because of structural loading, shrinkage (if the shrinkage is restrained), chemical attack, and thermal deformations. The tensile strength of concrete is only approximately 10% of its compressive strength, and brittle concrete cracks when subjected to tensile stresses. In addition to the mechanical properties, durability is vitally important for all concrete structures, and can generally be associated with the brittle nature of concrete.

In recent years, the effort to modify the brittle nature of ordinary concrete has resulted in modern concepts of ultrahigh performance fiber-reinforced cementitious composites (UHP-FRCC), which are characterized by tensile strain-hardening after first cracking. Depending on its composition, its tensile strain capacity can be up to several hundred times those of normal and fiber-reinforced concrete. Engineered cementitious composites (ECC) is a special type of UHP-FRCC designed based on micromechanical principles to strain-harden in tension. It allows optimization of the composite for high performance represented by extreme ductility while minimizing the amount of reinforcing fibers, typically less than 2% by volume (Li 1998; Li 2003; Li et al. 2001). Although various fiber types have been used in the production of ECC, polyvinyl alcohol (PVA) fiber was adopted in the current version of ECC. The use of PVA fiber was decided based on the composite performance and economics consideration, and PVA-ECC represents the most practical ECC used in the field at the present (Li et al. 2001; Kunieda and Rokugo 2006). Unlike other concrete materials, PVA-ECC strain-hardens after first cracking, similar to a ductile metal, and demonstrates a strain capacity up to 500 times greater than normal concrete. Tensile strain capacities of 2 to 5% have been easily produced in the field with materials and equipment commonly used in the concrete industry (Lepech and Li 2008). Unlike ordinary concrete and most fiber-reinforced concretes, ECC also exhibits self-controlled crack widths under increasing load. Even at large imposed deformation, crack widths of ECC remain small, less than 60 μm. With intrinsically tight crack width and high tensile ductility, ECC represents a new concrete material that offers significant potential to naturally resolve the durability problem of concrete structures.

Mineral admixtures such as fly ash (FA), silica fume, and ground granulated blast furnace slag improve the engineering properties of concrete when they are used as a mineral additive or partial replacement of cement. Among these mineral admixtures, FA is a finely divided residue of the very fine ash that is a by-product of the combustion of powdered coal in power plants. A recent development in the production of ECC has been to use FA as a partial replacement for portland cement in the production of ECC

[1]Associate Professor, Dept. of Civil Engineering, Gaziantep Univ., Gaziantep, Turkey (corresponding author). E-mail: sahmaran@gantep.edu.tr

[2]Postdoctoral Fellow, Ryerson Univ., Dept. of Civil Engineering, Toronto, and Assistant Professor, Dept. of Civil Engineering, Mustafa Kemal Univ., Iskenderun, Hatay, Turkey.

[3]Ph.D. candidate, Dept. of Civil Engineering, Gaziantep Univ., Gaziantep, Turkey.

[4]Professor, Ryerson Univ., Dept. of Civil Engineering, Toronto.

[5]Professor, Dept. of Civil and Environmental Engineering, Univ. of Michigan, Ann Arbor, MI.

Note. This manuscript was submitted on February 4, 2011; approved on May 6, 2011; published online on May 7, 2011. Discussion period open until May 1, 2012; separate discussions must be submitted for individual papers. This paper is part of the ***Journal of Materials in Civil Engineering***, Vol. 23, No. 12, December 1, 2011. ©ASCE, ISSN 0899-1561/2011/12-1735–1745/$25.00.

(Wang and Li 2007; Yang et al. 2007; Şahmaran and Li 2009). The addition of FA to ECC alters the microstructure of the composites. The changes in microstructure improve robustness (more consistent) of tensile ductility while retaining a long-term tensile strain of approximately 3% and reducing the crack width from approximately 60 to 10–30 μm or sometimes even lower than 10 μm (Wang and Li 2007).

High-volume fly ash (HVFA) PVA-ECC has been adopted in North America, Europe, and Asia for high-rise buildings, bridges, tunnels, highways, and other forms of infrastructure (Univ. of Michigan, ACE MRL 2008). Fire remains one of the primary threats to reinforced concrete structures, and the increasingly intensive use of HVFA-ECC in the construction industry makes it necessary to fully understand the effects of fire on the material. Although the residual mechanical properties of standard ECC mixture (also kown as ECC M45, with FA and cement ratio of 1.2) after exposure to high temperatures have been studied and obtained similar or better performances than those of plain concrete and fiber-reinforced concrete (Şahmaran et al. 2010), the influence of HVFA and micro PVA fiber on fire and spalling resistance has not yet been studied. Previous studies have shown that the fire resistance of conventional concrete is highly dependent on its constituent materials, particularly the mineral admixtures and fiber (Phan 1996; Yigang et al. 2000; Sarvaranta and Mikkola 1994a; Sarvaranta and Mikkola 1994b; Nishida et al. 1995). PVA synthetic fibers in ECC may also melt and leave a pathway for steam to escape, thereby contributing to the creation of a network more permeable than the matrix, which allows the outward migration of gas and results in the reduction of pore pressure and tendency to spall.

This study was undertaken to obtain more information on the fire resistance of ECC, particularly on the influence of micro PVA fiber and HVFA. ECC mixtures with two different FA to portland cement (FA/C) ratios (1.2 and 2.2) were prepared. To determine the effect of microfibers and ultrahigh ductility of ECC, ECC matrix mixtures of the same composition but without PVA fibers were also produced and tested for fire resistance. The role of PVA fibers and FA was analyzed in terms of physical and mechanical properties, microstructure, and fiber-matrix interactions as a function of heat treatment by using surface characterization, mass loss measurement, stress-strain measurement, mercury intrusion porosimetry, and scanning electron microscopy analysis.

Research Significance

ECC is a unique class of a new generation high-performance fiber-reinforced cementitious composites featuring high ductility and medium fiber content. With the current high volume use of FA in ECC mixtures incorporating PVA fiber, and the rise of fire hazards in infrastructure in recent years, a thorough understanding of the effect of FA content and PVA fiber on the fire resistance of ECC is urgently needed. Because ECC contains PVA fiber and more FA than conventional concrete, it is not known whether the fire resistance of HVFA-ECC is the same as conventional concrete. This research adds important data to existing information on the behavior of ECC under elevated temperatures.

Table 1. Mixture Properties of ECC

Mix ID		Ingredients (kg/m^3)							
		Cement	FA	Water	PVA	Sand	HRWR	FA/C	W/CM
ECC1	with fiber	558	669	326	26	446	2.3	1.2	0.27
	without fiber	558	669	326	—	446	2.3	1.2	0.27
ECC2	with fiber	375	823	318	26	435	2.0	2.2	0.27
	without fiber	375	823	318	—	435	2.0	2.2	0.27

Experimental Studies

Materials, Mixture Proportions, and Basic Mechanical Properties

ECC mixtures with FA/C ratios of 1.2 and 2.2 by weight (55 and 70% by weight of total cementitious materials) were used in this investigation, details of which are given in Table 1. Type I ordinary portland cement (C), fine silica sand with an average grain size of 110 μm, Class-F FA conforming to ASTM C618 (1994) requirements, PVA fibers, and a polycarboxylate-based high range water reducer (HRWR) were used. The chemical compositions and physical properties of the cement and FA are reported in Table 2. The PVA fibers had an average diameter of 39 μm, average length of 12 mm, a tensile strength of 1,600 MPa, a density of 1,300 kg/m^3, an elastic modulus of 42.8 GPa, and a maximum elongation of 6.0%. Additionally, because of the strongly hydrophilic nature of PVA, the fiber surfaces were coated with an oiling agent (1.2% by weight) to reduce the interfacial bond strength between the fiber and matrix.

The spalling of concrete under high temperatures is a concern owing to exposure of the steel reinforcement to direct fire contact and subsequent structural capacity loss of the element. The most commonly used solution to avoid spalling is adding low melting-point synthetic [mostly polypropylene (PP)] fibers. The inclusion of PP fibers reduces the likelihood of concrete spalling at high temperatures because water vapor can exit through channels created by the melted fibers (Sarvaranta and Mikkola 1994a; Sarvaranta and Mikkola 1994b; Nishida et al. 1995). Although various fiber types have been used in the production of ECC, PVA fiber was adopted in the current version based on composite performance and economic consideration. PVA synthetic fibers in ECC may behave similarly to PP fibers—they may also melt and leave sufficient space for steam to escape—thereby avoiding internal pressure buildup and associated cover bursting. To analyze the influence of micro PVA fibers on fire resistance of ECC, matrix mixtures (in this study, the term "matrix" is used to identify ECC mixture without PVA fiber) were also studied (Table 1). The ECC (with fiber) and matrix (without fiber) mixtures were prepared in a standard mortar mixer at a constant amount of cementitious material (C + FA) and constant water to cementitious material (W/CM) ratio of 0.27. HRWR was added to the mixture until the desired fresh ECC characteristics, described in another study (Yang et al. 2009), were visually observed. Based on this study, it is recommended that a W/CM ratio in the range of 0.25 ± 0.05 be adopted in an ECC mix with uniform fiber distribution, and a high plastic viscosity

Table 2. Properties of Cement and Fly Ash

	Chemical composition (%)									Physical properties		
	CaO	SiO_2	Al_2O_3	Fe_2O_3	MgO	SO_3	K_2O	Na_2O	LOI	Spec. grav.	Ret. on 45 μm (%)	Water req. (%)
C	61.8	19.4	5.3	2.3	0.95	3.8	1.1	0.2	2.1	3.15	12.9	—
FA	5.57	59.5	22.2	3.9	—	0.2	1.11	2.75	0.2	2.18	9.6	93.4

Table 3. Compressive and Uniaxial Tensile Properties of ECC Specimens

Specimen	Compressive strength (28-day) (MPa)		Tensile strain (%)		Tensile strength (MPa)		Residual crack width (μm)	
	with fiber	without fiber	14-day	28-day	14-day	28-day	14-day	28-day
ECC1	62.5	60.3	2.91 ± 0.22	2.73 ± 0.24	4.63 ± 0.48	5.14 ± 0.31	~60	~48
ECC2	54.1	52.4	3.24 ± 0.14	3.02 ± 0.19	4.17 ± 0.36	4.82 ± 0.27	~40	~30

(high Marsh cone flow time) and a low yield stress (high minislump flow diameter) be achieved through adjustment of the amount of HRWR.

Table 3 shows compressive strength test results of the ECC and ECC matrix mixtures and the tensile behavior of ECC mixtures cured in an environmental chamber at a temperature of 23 ± 2°C and a relative humidity of $95 \pm 5\%$ until the age of testing. The compressive strength was computed as an average of three 50 mm cube specimens. As shown in Table 3, and as expected, the compressive strength of ECC decreased with increasing FA content. However, even at almost 70% replacement of portland cement with FA (FA/C = 2.2), the compressive strength of ECC at 28 days can be greater than 50 MPa. Moreover, because of the delay in hydration when very high FA contents are used, the compressive strength of HVFA-ECC is expected to increase significantly in the long term (Şahmaran et al. 2007).

To characterize the direct tensile behavior of the ECC mixtures, $200 \times 75 \times 13$ mm coupon specimens were used. Direct tensile tests were conducted under displacement control at a loading rate of 0.005 mm/s. The typical tensile stress-strain curves of the ECC mixtures at 28 days are shown in Fig. 1. Four specimens were tested for each mix and for each age. As shown in Table 3, the ECC composites exhibited a strain capacity of more than 2.7% at 28 days. Previous studies demonstrated that the tensile strain capacity seems to stabilize after 28 days (Wang and Li 2007; Yang et al. 2007; Şahmaran and Li 2009). As shown in Table 3, the increase of FA/C ratio improves the tensile strain of ECC. The improvement in the tensile strain with the increase in the FA content could be because increase in the FA content tends to reduce the PVA fiber/matrix interface chemical bond and matrix toughness while increasing the interface frictional bond in favor of attaining high tensile strain capacity (Wang and Li 2007). On the other hand, the increase in the FA content slightly influenced the tensile strength, which is above 4.0 MPa. Table 3 gives also the effect of FA content on the residual crack width at different ages. The crack width was found to reduce significantly as FA content increases at all ages. The reason for this is likely associated with the higher fiber/matrix interface frictional bond with the increase of FA volume (Wang and Li 2007; Yang et al. 2007).

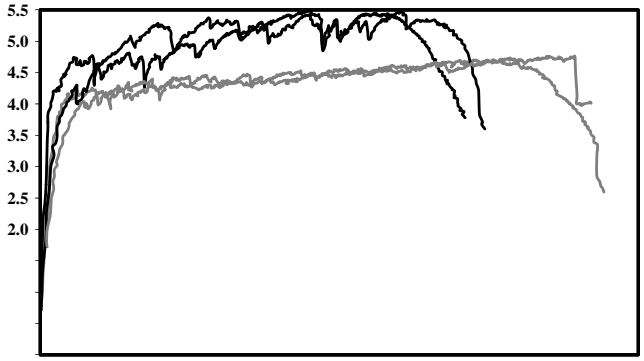

Specimen Preparation and Testing

Fire Resistance

Several 50 mm cubes from ECC (with fiber) and ECC matrix (without fiber) were cast to determine residual mechanical and microstructural properties. Specimens were demolded 24 h after casting and conditioned in an environmental chamber at a temperature of 23 ± 2°C and a relative humidity of $95 \pm 5\%$ until the age of 28 days. From each mixture, six cubes were tested under compression immediately after conditioning at 28 days; these control specimens will be referred to as those tested after exposure to normal curing condition (unheated). The remaining specimens were heated to targeted temperatures at 28 days, and their residual properties were then investigated. The heating equipment used in the investigation was a computer-controlled, electrically heated furnace. In the furnace, cubes were heated at a constant rate of approximately 15°C/min to reach the prescribed temperatures. Four maximum temperatures (200, 400, 600, and 800°C) and exposure periods were chosen in accordance with other published studies (Chan et al. 1999; Chan et al. 2000; Poon et al. 2003; Xu et al. 2001; Xu et al. 2003). When the targeted peak temperature was reached, the furnace temperature was maintained constantly for 60 min to achieve the thermal steady state (Mohamedbhai 1986). After that, the samples were allowed to cool naturally to room temperature.

After the specimens had been allowed to cool naturally to room temperature, residual compressive strengths were determined on ECC specimens subjected to high temperatures ranging from 200 to 800°C. An axial load was performed under displacement control at a loading rate of 0.005 mm/s on a closed-loop controlled servohydraulic material test system with 200-kN capacity. During the compressive tests, the load and deflection values were recorded on a computerized data recording system. Six specimens were tested for each stage and average values were recorded. The weight of each specimen was also measured before and after exposure to calculate the mass loss of fire-deteriorated specimens.

Microstructure Characterization

It is generally accepted that the mechanical properties of any material are always closely linked to its pore structure. The pore structure controls water expulsion from concrete at both normal and elevated temperatures. Thus, to a certain degree, the variation in pore structure reflects the deterioration of materials subjected to high temperatures. In this study, mercury intrusion porosimetry (MIP) was used to identify the changes occurring in the porosity and pore size distribution of hardened ECC control (unheated) specimens and specimens subjected to various elevated temperatures. In all cases, at least two identical ECC specimens were tested at the same time. Studying the pore structure of concrete after high-temperature exposure helps to understand the mechanisms of deterioration. The microstructure of specimens was also investigated using scanning electron microscope (SEM) observation. The results of the microscopic investigations gave a good explanation of

the change in macro behavior of ECC in comparison to ECC matrix mixtures.

Experimental Results and Discussions

SEM Observations, Porosity, and Pore Size Distribution

To study the behavior of fibers and matrix microstructure after various elevated temperatures, observations with an SEM were performed on samples taken from the cores of 50 mm ECC specimens that had been exposed to a temperature between 200 and 800°C for one hour. Because matrix (ECC without fiber) specimens had severely deteriorated as a result of heat exposure at temperatures over 200°C, microstructural studies were not performed for heated ECC matrix specimens.

Fig. 2 shows the SEM micrographs of ECC specimens for the unheated specimens and the thermally treated specimens at various temperatures. Fig. 2(a) shows general view of PVA fibers scattered in a nonheated ECC specimen. Micrographs of the unheated samples consist primarily of ill-crystallized and fibrous particles of calcium-silicate-hydrate (CSH) gel, amorphous and well-crystallized calcium hydroxide, and numerous unhydrated FA particles. Fig. 2(b) shows that the microstructure of the ECC specimen did not undergo significant changes, because it shows no apparent cracks after fire exposure at 200°C. At 400°C, PVA fibers melt completely, creating additional interconnected pores and small channels in the matrix that can decrease pore pressure inside the ECC [Fig. 2(c)]. As shown in Fig. 2(c), PVA fiber count (influenced by dosage and diameter) is high enough that fibers alone constitute a connected network. Therefore, the use of PVA fiber clearly affects porosity at high temperatures. After exposure to 600 and 800°C, the morphology of hydration products showed numerous intact FA particles and massive structure of hydration products (especially CSH gel); almost all hydration products appearing as ill-crystallized or amorphous structures by losing their characteristic crystal structure [Fig. 2(d)]. SEM analysis also indicated that beyond 800°C, microcracking increased around the grains of unhydrated FA particles and silica sand lost their characteristic structure [Figs. 2(d) and 3].

The deterioration of ECC's structural integrity when exposed to various temperatures is also illustrated by an average pore diameter and porosity increase in Tables 4 and 5. Fig. 4 provides the variations of cumulative pore volume and its distribution, as influenced by different heating regimes. Before exposure to high temperature, the major difference between the ECC and ECC matrix mixtures existed in the macropores with diameter greater than approximately 0.30 μm (Table 4). Additionally, there is little difference between ECC1 and ECC2 mixtures. After being subjected to various high temperatures, as shown in Table 5, the higher the temperature, the coarser the pore structure and the higher the total intruded porosity of ECC mixtures. The variation of both ECC1 and ECC2 was very similar; consequently, their relative residual strengths should be similar. In terms of total intruded porosity and coarsening effect (average pore diameter), the changes appeared more rapidly with temperatures over 600°C. The average pore diameter dramatically enlarges to 2–10 times its original size after ECC has been exposed to 600 and 800°C, respectively.

The MIP test results highlight pore structure coarsening and increase in total intruded porosity at elevated temperatures; these are the major reasons for the strength and stiffness losses, discussed in a later section. After exposure up to 400°C, the MIP test results given in Fig. 4 indicate that ECC showed reduction in the cumulative volume of pores larger than 0.1 μm, which generally influences the strength of the concrete (Rostasy et al. 1980). The reduction of cumulative volume of pores larger than 0.1 μm may be attributable to further hydration of unhydrated cement

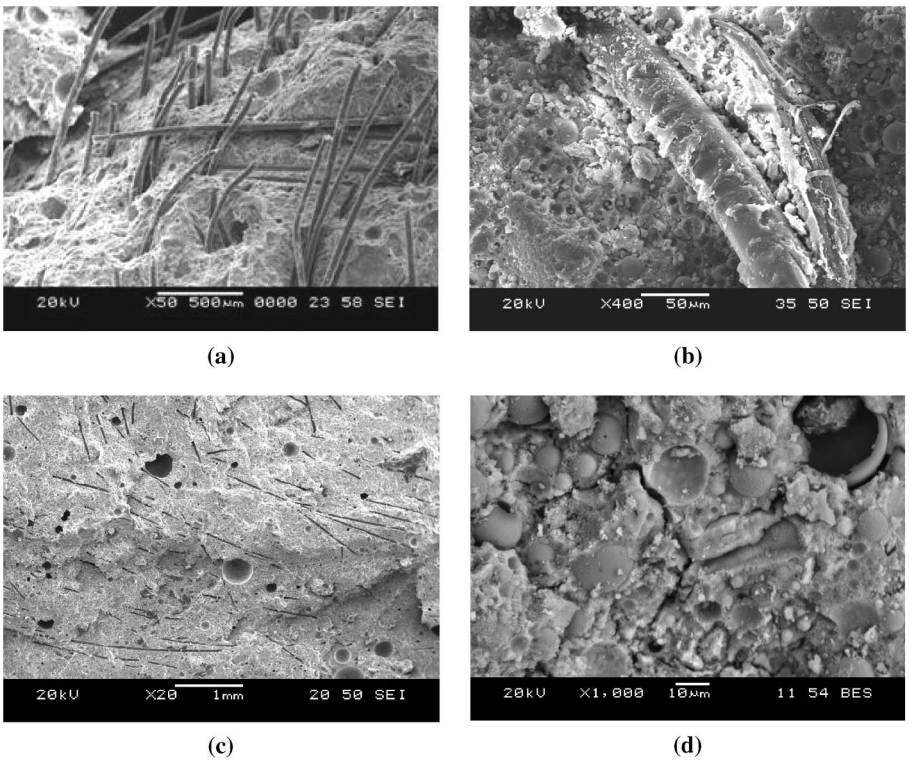

Fig. 2. SEM micrograph of ECC before and after thermal treatment: (a) control (unheated); (b) after 200°C heat treatment; (c) after 400°C heat treatment; (d) after 800°C heat treatment

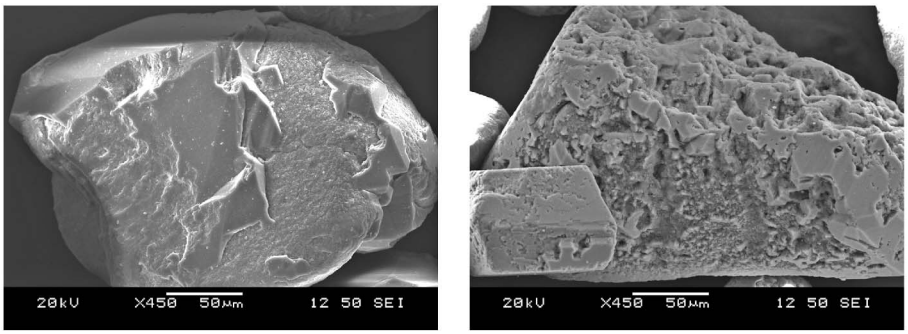

Before heat treatment **After 800 °C heat treatment**

Fig. 3. SEM micrograph of silica sand before and after thermal treatment

particles and the pozzolanic reaction of unhydrated FA particles with free lime to produce more CSH phases that deposit in the pore system (Khoury 1992). Because the coarsening of ECC was not significant in this temperature range, the strength and stiffness loss occurred at temperatures up to 400°C might be attributed to internal microcracking, which is evident from some SEM micrographs. This was probably attributable to the very dense internal structure of ECC, which results in an increased vapor pressure formed by the evaporation of free physically bonded water, and the dissociation of calcium hydroxide (CH) crystals, followed by high tensile stresses. The reason for the dense microstructure of the ECC mixture can be attributed to a significantly low W/CM ratio, high cementitious materials content, and an absence of coarse aggregate.

As shown in Fig. 4, the cumulative volume of pores larger than 0.1 μm greatly increased after exposure to temperatures of 600°C and above. This was an important factor deemed to be responsible for strength deterioration in ECC mixtures after heat exposures to temperatures of 600°C. The degradation of hydrates (CSH gels), which is inevitable when the exposure temperature is raised to 600°C (Khoury et al. 1985), is the primary reason for severe pore structure coarsening. After exposure to the high temperature of 800°C, the average pore diameter of both ECC1 and ECC2 mixtures increased significantly, in which ECC2 had the largest increase by 910%, and the porosity of ECC1 was smaller than that of ECC2. Interestingly, despite the higher porosity and similar or higher increase in relative residual average pore diameter, ECC2 showed significantly lower strength and stiffness losses than those of the corresponding ECC1 mixture after heat exposure (discussed in a following section).

Table 4. Pore Size Distribution of ECC and ECC Matrix Mixtures

	ECC1 (M45)		ECC2 (M45)	
Pore diameter (μm)	with PVA	without PVA	with PVA	without PVA
Volume of pores $>$ 0.30	5.00	0.76	5.14	1.38
Volume of pores $<$ 0.30	18.70	18.48	22.08	23.06
Total intruded porosity	23.70	19.24	27.22	24.44

Surface and Spalling Characteristics and Mass Loss

Spalling is a catastrophic failure of concrete that generally occurs during a fire, and is characterized by explosive fracture and ejection of pieces of the material, often without prior warning. The ability of concrete to withstand high temperatures can be hampered considerably by spalling. Spalling may cause loss of the concrete cover, resulting in direct exposure of reinforcing bars to high temperatures that severely reduce the structural integrity and bearing capacity of the reinforced concrete structure. One of the primary mechanisms responsible for concrete spalling is thought to be the vapor pressure buildup (Chan et al. 1999) when pore water turns into steam if no escape channels are available. Previous studies have demonstrated that spalling in concrete occurs between 190 and 250°C (Kalifa et al. 2000).

In this study, explosive spalling and splitting/cracking were observed only in ECC matrix (without fiber) specimens, whereas no spalling occurred after ECC specimens were subjected to air cooling after being exposed to peak temperatures of up to 800°C. Spalling occurred in ECC matrix specimens at 400°C and above, with more frequency at 600°C (Fig. 5). Based upon this evaluation,

Table 5. Total Intruded Porosity and Average Pore Diameter of ECC Samples after Subjection to Various Temperatures

Specimen		ECC1 (M45)		ECC2	
		without fiber	with fiber	without fiber	with fiber
Control (23°C)	Total intruded porosity (%)	19.2	23.7	24.4	27.2
	Average pore diameter (nm)	10.8	12.1	13.7	14.1
200°C	Total intruded porosity (%)	—	23.9 (0.8)[a]	—	29.1 (7.0)
	Average pore diameter (nm)	—	13.4 (10.7)	—	16.6 (17.7)
400°C	Total intruded porosity (%)	—	28.6 (20.7)	—	31.0 (14.0)
	Average pore diameter (nm)	—	18.2 (50.4)	—	17.8 (26.2)
600°C	Total intruded porosity (%)	—	32.0 (35.0)	—	31.6 (16.2)
	Average pore diameter (nm)	—	31.9 (163.6)	—	26.5 (87.9)
800°C	Total intruded porosity (%)	—	32.4 (36.7)	—	34.4 (26.5)
	Average pore diameter (nm)	—	113.6 (838.8)	—	142.5 (910.6)

[a]Numbers in parentheses indicate relative residual porosity and average pore diameter in percentage.

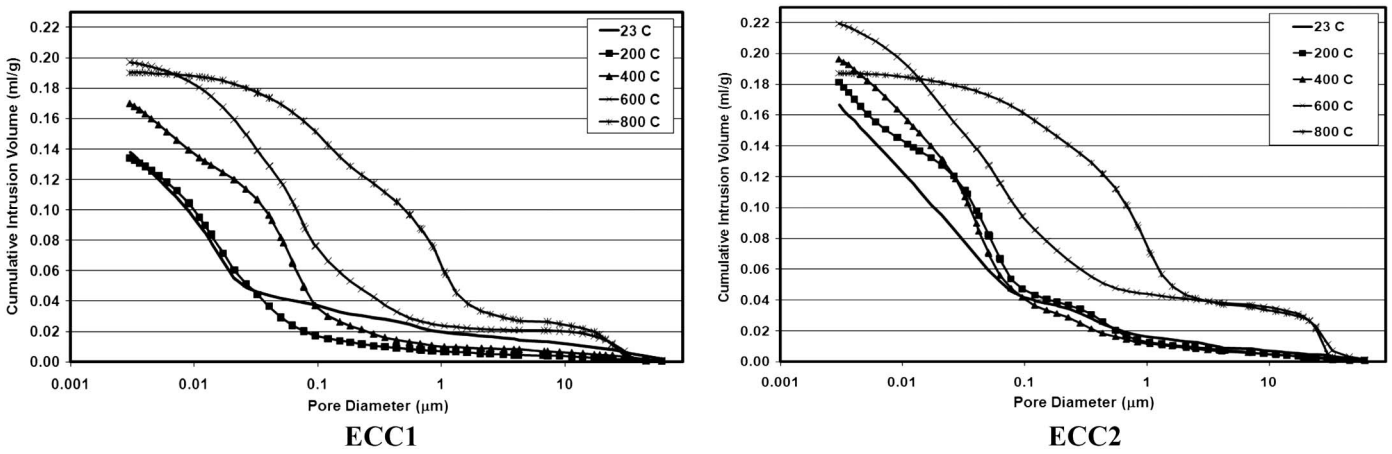

Fig. 4. Pore size distributions of ECC before and after exposure to high temperatures

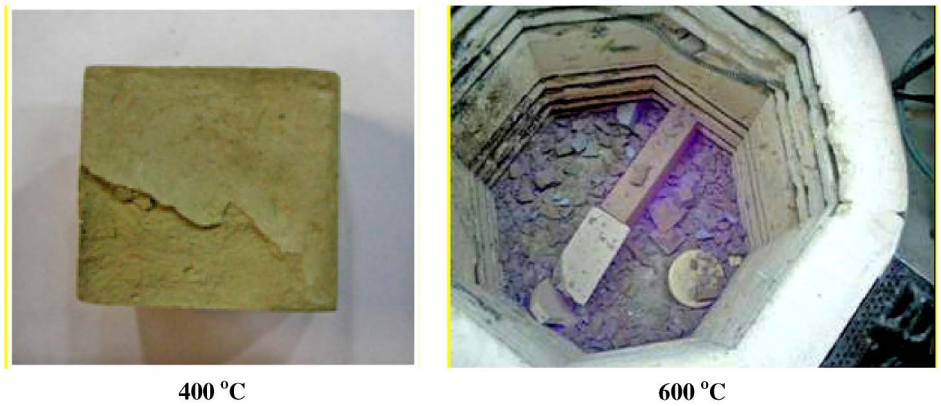

Fig. 5. Cracking of ECC matrix cubic specimens after exposure to 400 and 600°C

the obvious reason may be the dense pore structure of ECC matrixes that held the vapor pressure of steam and resulted in explosive spalling. This was verified from the results of MIP analysis, which indicated a lower porosity in ECC matrixes than corresponding ECC mixtures. Because explosive spalling is governed by a vapor-pressure mechanism (Chan et al. 1999), it is reasonable to consider that concrete incorporating PVA fiber can provide a benefit to ECC that prevents it from explosive spalling, because it is melted under temperatures at approximately 230°C, and hence, moisture in ECC can escape through interconnected pores to outside of ECC (Şahmaran et al. 2010).

Fig. 6 shows surface crack patterns of ECC specimens as a result of various elevated temperatures. Cracking became apparent when the exposure temperatures exceeded 400°C. In some of the cubes, hairline cracks were observed at 400°C [Fig. 6(b)]. At temperatures above 400°C, microcracking increased significantly [Figs. 6(c) and 6(d)], first around hydration products and then around grains of unhydrated FA and cement.

The deterioration of specimens subjected to various elevated temperatures was also assessed by mass loss measurements. Fig. 7 shows the relation between weight loss and temperature of heated ECC and ECC matrix mixtures. As shown in Fig. 7, the mass loss increased with increasing exposure temperature, a result that is primarily associated with the liberation of free and physically bound water from the decomposition of calcium hydrates and the other formed cement hydrates. At higher temperatures of 600 and 800°C, the weight change of ECC was primarily caused by the dehydration of paste and crystal transformation of quartz, as discussed in the preceding section. During heat treatment up to 400°C, the weight of the melted fibers also had an influence on mass loss, although this loss is probably insignificant (less than 1.5%) compared to the observed total loss of over 10%.

Residual Mechanical Properties

To predict the mechanical behavior of ECC and ECC matrix mixtures after exposure to elevated temperatures, the compressive strength of test specimens was measured shortly after heating, when specimens had cooled to room temperature. The results of compressive strength of fire-deteriorated specimens are given in Table 6. In the table, each value represents the average test result of six specimens. Complete stress-strain curves of both the unheated and heated specimens were also obtained from compression tests, with a displacement control rate of 0.005 mm/s on a closed-loop controlled servohydraulic material test system. The typical compressive behavior of the tested specimens is presented in Fig. 8. The axial strains of concrete in compression were obtained from full-height shortening of the cubic specimens using LVDTs. Such strains are generally larger than those obtained at the midheight region because of the end effects (Lam et al. 1998). The typical compressive stress-strain curves of ECC specimens after thermal deterioration show that the influence of elevated temperatures up to 400°C on compressive properties is fairly minor (Fig. 8). This

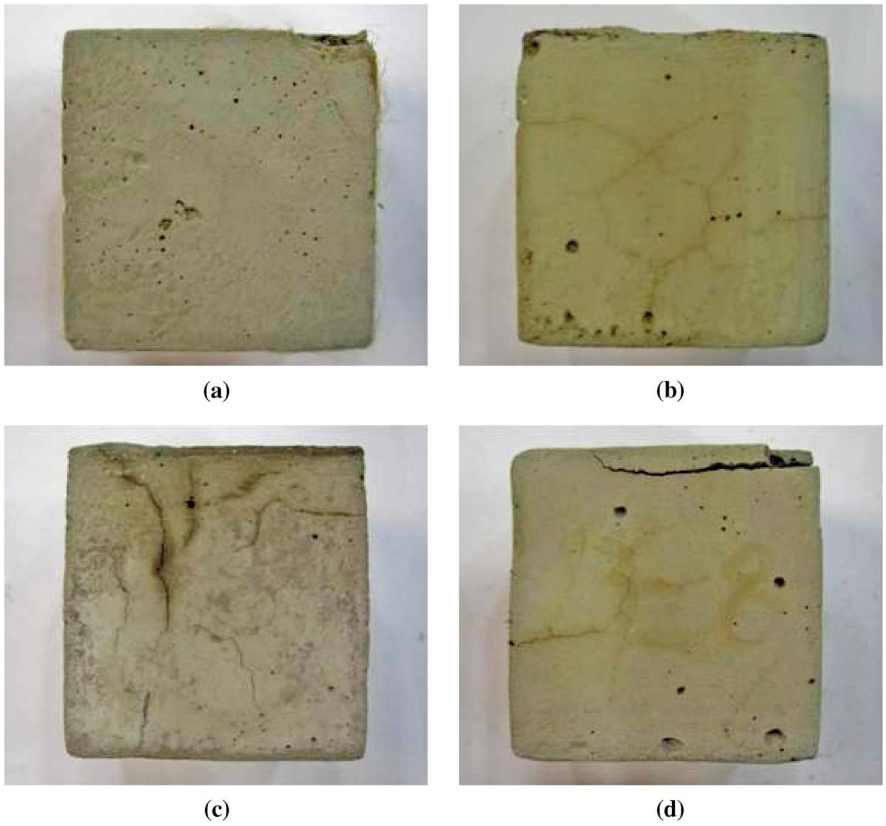

Fig. 6. Typical crack patterns on the surface of ECC cubic specimens after exposure to high temperatures: (a) 200°C; (b) 400°C; (c) 600°C; (d) 800°C

result is consistent with the results of microstructural analysis of ECC specimens reported in the previous section.

The slope of the load-deflection curve represents the stiffness of the specimens. Fig. 8 shows that the slope decreases with the increase in exposure temperature up to 800°C, indicating a reduction in the stiffness of the ECC cube specimens. The figure also shows that after exposure to elevated temperatures, the initial ascending parts of the curve for the ECC were approximately linear, but the stiffness magnitudes were much lower. The decrease in stiffness (in percentage) with increasing temperature is summarized in Table 6, where the ECC stiffness data were obtained within 30% of the ultimate strength, and were given as relative values with reference to the elastic modulus of the unheated ECC mixes.

Fig. 9 shows the effect of temperature on the residual compressive strength and stiffness of the ECC and matrix mixtures. The residual strength and stiffness percentages were the ratios of the strength and stiffness of samples that were exposed to high temperature to that of the relative control (unheated) samples. As shown in Fig. 9, from the perspective of residual compressive strength of ECC, the heating regime can be divided into two ranges, namely 23–400°C and 400–800°C. In the range 23–400°C, the ECC mixtures showed slight losses in their original compressive strength. This decrease may be attributed to internal microcracking. After exposure to a higher temperature of 200°C, ECC2 (FA/PC = 2.2) exhibited a much better fire resistance than ECC1 from the viewpoint of strength loss; however, the former still had considerable

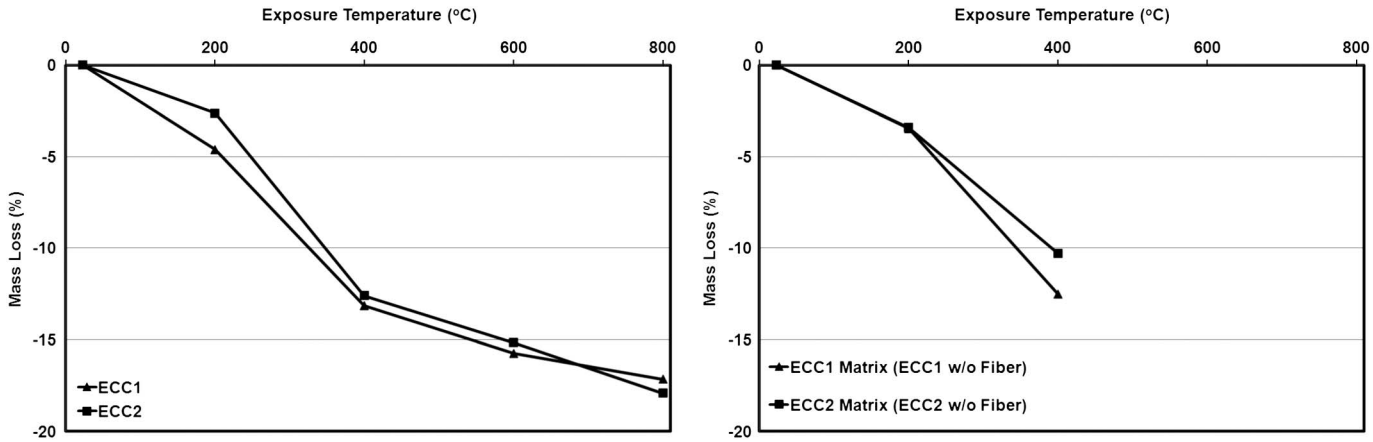

Fig. 7. Change in mass loss of ECC and ECC matrix mixtures with temperature

Table 6. Effect of Temperature on Compressive Strength and Relative Stiffness

	Compressive strength (MPa)				Relative stiffness (%)			
Specimen	ECC1 without fiber	ECC1	ECC2 without fiber	ECC2	ECC1 without fiber	ECC1	ECC2 without fiber	ECC2
23°C	60.2	64.3	52.9	51.8	100.0	100.0	100.0	100.0
200°C	54.0	55.2	51.9	50.0	80.7	84.7	87.7	94.1
400°C	40.1	54.9	44.1	49.4	54.2	66.3	66.3	82.5
600°C	—	34.2	—	33.1	—	35.5	—	51.3
800°C	—	21.6	—	19.8	—	21.9	—	28.5

residual mechanical properties. Only a negligible proportion of the original strength was lost for ECC2; the loss was no more than 5%. Relatively high residual compressive strength of ECC2 (FA/C = 2.2) specimens at 200°C is probably because of the hydration of unhydrated FA particles with free lime, which were activated as a result of temperature rise. Because the hydration in ECC incorporating higher FA volume is slowed down after 14 days owing to the blocking of capillaries, such a good performance in strength at elevated temperatures can be anticipated. A similar result in strength was observed in concrete incorporating mineral admixtures because of the formation of tobermorite (Nasser and Marzouk 1979; Poon et al. 1999).

Fig. 9 shows that as temperature increases from room temperature up to 400°C, the compressive strength of ECC mixtures drops slightly, followed by minimal microcracking on the surface, when compared to ECC specimens after initial heating up to 200°C. In general, compressive strength might be considered a constant. The constant compressive strength evident between 200 and 400°C—despite significant loss of weight and increase in porosity—is an interesting phenomenon. The increase in porosity is most likely because of the additional porosity and small channels created in the ECC by melting PVA fibers. Despite the increase in total intruded porosity, the average pore diameter of ECC matrix (coarsening) shows little change up to 400°C. Fortunately, the hardening effect can almost compensate for the loss of strength caused by the coarsening and increase in porosity of the ECC matrixes and the weakening of the interfacial transition zone. Also, no spalling occurred in this temperature range. On the other hand, when the temperature reaches 400°C, both ECC1 and ECC2 matrix mixtures (without fiber) showed a sharp reduction in their original compressive strength followed by explosive spalling and severe cracking (Figs. 5 and 9). The compressive strength tests could not proceed because the

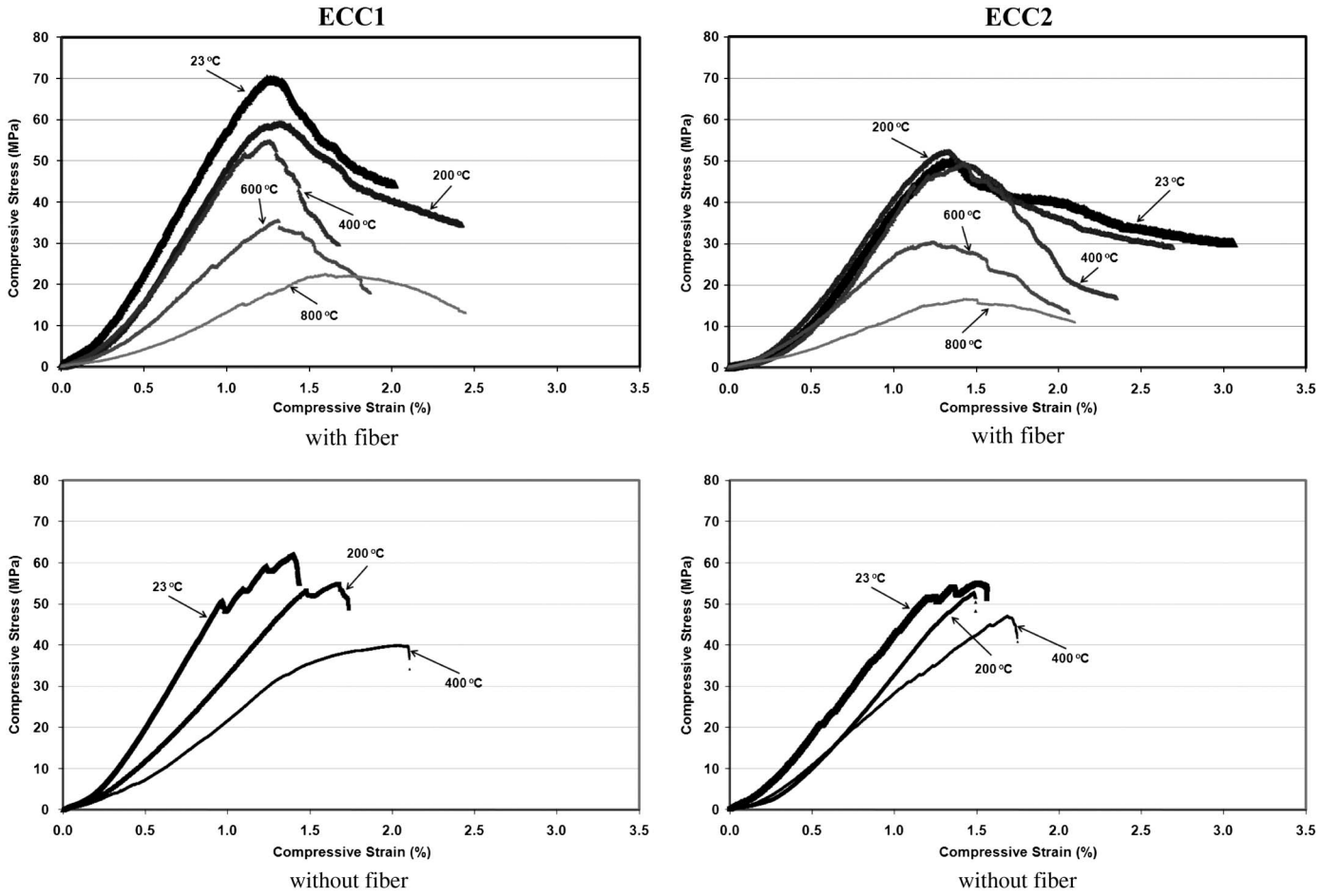

Fig. 8. Effect of elevated temperatures on compressive stress-strain curves of ECC and ECC matrix mixtures

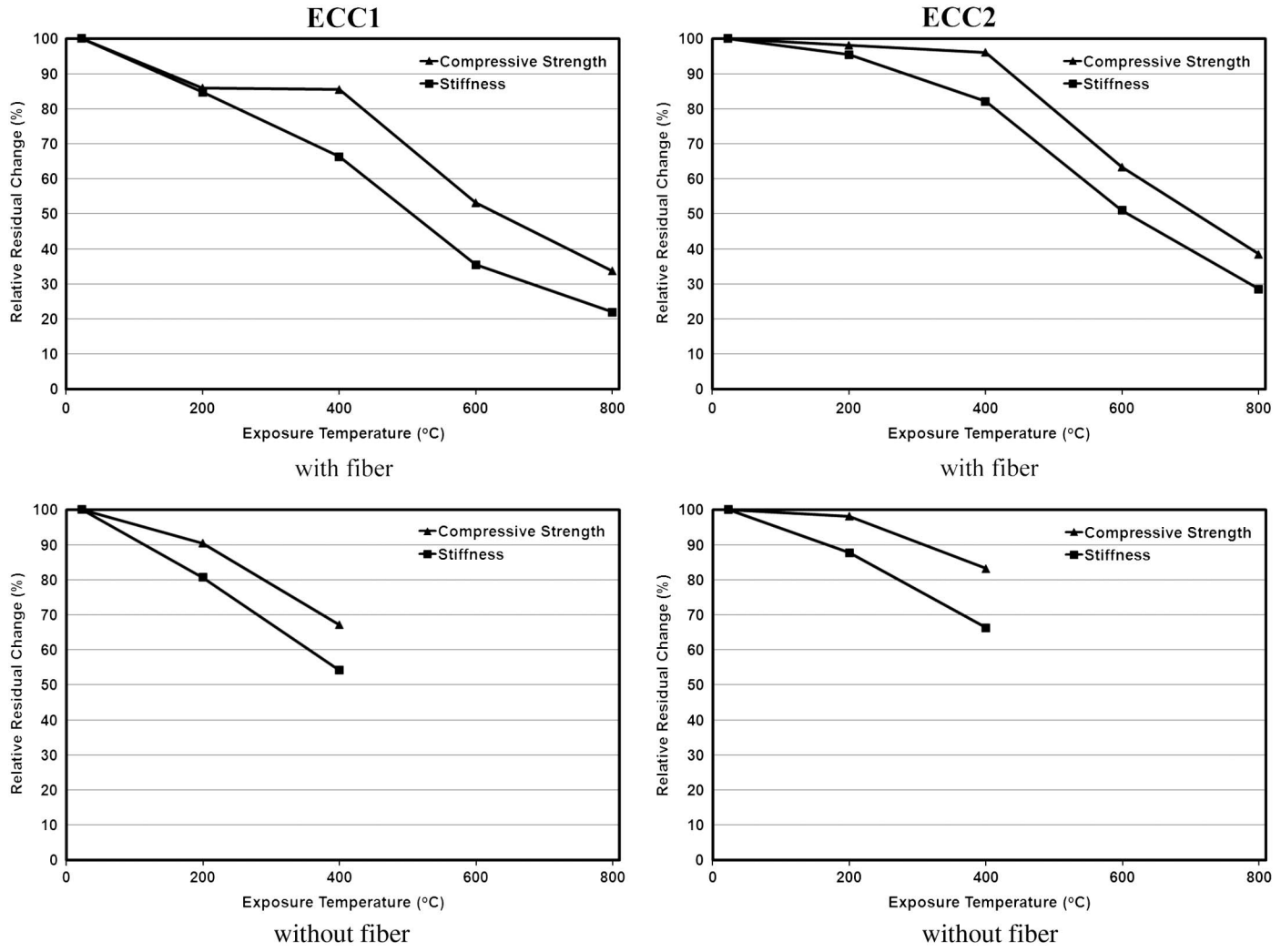

Fig. 9. Degradation of ECC in terms of compressive strength and stiffness as a function of exposure temperature

cracking was too severe and assessing the mechanical properties of matrix mixtures of ECC exposed to such a temperature higher than 400°C became meaningless.

In light of this point, PVA fiber is beneficial in helping ECC overcome vapor pressure buildup under high temperatures, and hence, avoiding occurrence of spalling by melting at approximately 230°C. Therefore, incorporating PVA fiber seems to be a promising way to enhance the resistance of matrix to thermally induced explosive spalling, which was experimentally confirmed by this investigation. Water vapor in ECC can escape through interconnected channels without creating detrimental internal pressure. The plateau in compressive strength between 200 and 400°C may also be linked to the fact that, despite the increase in total intruded porosity, the average pore diameter of ECC matrix shows little change up to 400°C. Test results also seemed to denote that the PVA fiber did not necessarily lead to a reduction in strength after vaporized at high temperature. Previous research on plain high-performance concrete (HPC) and fiber-reinforced concrete indicate similar trends up to 400°C (Gowripalan et al. 1997; Poon et al. 2004).

At 400°C or more, the loss in stiffness is considerably sharp, which is clearly different from the more gradual loss of compressive strength up to 400°C heat exposure. This is because heating to 400°C generates a relatively insignificant amount of microcracking and a significant amount of mass loss, and stiffness is more sensitive to mass loss and cracks either on the macroscale or microscale, which are caused by high temperatures to ECC (Wu et al. 2002; Xu et al. 2001; Xu et al. 2003). These did not cause any immediate loss of load carrying capacity in compression (Table 6), however, because of the lack of sensitivity of compressive strength to microcracks and moisture loss (Wu et al. 2002; Xu et al. 2003). This conclusion is confirmed by the stronger correlation that mass (or moisture) loss correlates with stiffness more than with compressive strength (compare Figs. 7 and 9).

In the range 600–800°C, these ECC mixtures lost most of their original strength, especially at temperature of 800°C. Thus, this temperature range may also be regarded as the critical temperature range for the strength loss of ECC. Even for an exposure temperature of 600°C, the beneficial effect of the high FA dosage was still significant, resulting in a residual compressive strength of 64% of the original unheated strength for ECC mixtures with FA/C ratio of 2.2 (ECC2), whereas only 53% of the original strength was maintained when the ECC1 (FA/C = 1.2) mixture was exposed to the same temperature. Therefore, the results showed a close correlation between the FA content and the degree of damage, because specimens with higher FA contents suffered a smaller loss. As indicated before by MIP analysis, this severe strength loss was because of the denser pore structure of ECC1, which enhanced more of the buildup of vapor pressure upon heating and resulted in spalling and cracking. The best performance at all temperatures, therefore, was given by ECC2 (ECC with FA/C ratio of 2.2). Recent studies

have also shown that the addition of FA can improve the residual compressive strength of cement paste; this improvement is especially significant for exposure temperatures above 400°C (Xu et al. 2003; Dias et al. 1990; Xu et al. 2001). CH decomposes after exposure to temperatures greater than 400–600°C (Taylor 1964), and the rehydration of dissociated CH becomes a detrimental cause of microcracking, accompanied by a 44% volume increase (Petzold and Rohr 1970). Therefore, the reduced calcium hydroxide in ECC matrix containing FA (which occurs as a result of pozzolanic reaction) may be an additional factor that leads to reduced cracking and improved mechanical properties (Xu et al. 2003; Dias et al. 1990; Xu et al. 2001). On the other hand, the effect of the addition of FA diminished when the exposure temperature was raised to 800°C.

Microstructural analysis revealed that the rapid degradation of mechanical properties at exposure temperatures up to 600°C is most likely attributable to the physical changes (increase in porosity, main pore radius of ECC matrix and cracking density) taking place in the matrix. After an exposure temperature of 600°C, the primary causes of deterioration in compressive strength and stiffness may be attributed both to the physical transformation of the matrix and chemical transformation of hydration products. When the temperature was raised to 600°C, decomposition of the major hydrate, tobermorite (gel), was inevitable (Khoury et al. 1985), causing severe increase in the microstructure of its matrix and the loss of binder property. Disintegration of fine silica sand also occurred at 800°C (Fig. 3). At the same time, dehydration went further at such an exposure temperature.

Conclusions

The objective of this research is to assess the effect of FA and micro PVA fibers on the fire durability of ECC. ECC mixtures with two different contents of FA as a replacement of cement (approximately 55 and 70% by weight of total cementitious material) were prepared. To find out the effect of PVA fibers on ECC, ECC matrix mixtures of the same composition except PVA fiber were also produced and tested for fire resistance. Mechanical properties (compressive strength, stress-strain relationship, and stiffness) and microstructural properties (mercury intrusion porosimetry and scanning electron microscopy analyses) of ECC and matrix mixtures were studied at room temperature and after exposure to temperatures up to 800°C for one hour.

When exposed to high temperatures up to 400°C, the residual properties of both ECC mixtures drop slightly, followed by minimal microcracking on the surface, when compared to values obtained from unheated specimens. On the other hand, at this temperature range (200 to 400°C) both ECC matrix mixtures (without fiber) showed a sharp reduction in their original compressive strength followed by explosive spalling and severe cracking. In light of this point, PVA fiber is beneficial in helping ECC overcome vapor pressure buildup under high temperatures and hence avoiding the occurrence of spalling by melting at approximately at 230°C. Therefore, incorporating PVA fiber seems to be a promising way to enhance the resistance of matrix to thermally induced explosive spalling, which was experimentally confirmed by this investigation. Moreover, no spalling occurred after ECC specimens were subjected to air cooling, even after being exposed to peak temperatures of up to 800°C. Increasing FA content from 55% to approximately 70% provide ECC with better residual mechanical properties after exposure to temperatures from 200 to 600°C. Thus, it may be feasible to increase the allowable working temperature for ECC by incorporating a high volume of FA into mixes, which means that a larger proportion of structures exposed to high temperatures can remain serviceable. On the other hand, the effect of the addition of FA diminished when the exposure temperature was raised to 800°C.

Acknowledgments

The authors gratefully acknowledge the financial assistance of the Scientific and Technical Research Council (TUBITAK) of Turkey provided under Project: MAG-108M495, Gaziantep University Scientific Research Centre provided under Project: MF.10.09, The Council of Higher Education of Turkey, and the Natural Sciences and Engineering Research Council (NSERC) of Canada, the Canada Research Chair Program. Support from the U.S. National Science Foundation (NSF CI-Team OCI 0636300) for international collaborative research on ECC is gratefully acknowledged.

References

ASTM. (1994). "Standard specification for coal fly ash and raw or calcined natural pozzolan for the use of mineral admixtures in portland cement concrete." *C618*, West Conshohocken, PA.

Chan, Y. N., Luo, X., and Sun, W. (2000). "Compressive strength and pore structure of high-performance concrete after exposure to high temperature up to 800°C." *Cement Concrete Res.*, 30(2), 247–251.

Chan, Y. N. S., Peng, G. F., and Anson, M. (1999). "Fire behavior of high performance concrete made with silica fume at different moisture contents." *ACI Mater. J.*, 96(3), 405–409.

Dias, W. P. S., Khoury, G. A., and Sullivan, P. J. E. (1990). "Mechanical properties of hardened cement paste exposed to temperatures up to 700° C (1292°F)." *ACI Mater. J.*, 87(2), 160–166.

Gowripalan, N., Salonga, P., and Dolan, C. (1997). "Residual strength of HPC subjected to high temperatures." *HPC: Design and materials and recent advances in concrete technology*, *ACI SP-172*, American Concrete Institute, Detroit, MI, 171–191.

Kalifa, P., Menneteau, F. D., and Quenard, D. (2000). "Spalling and pore pressure in HPC at high temperatures." *Cement Concrete Res.*, 30(12), 1915–1927.

Khoury, G. A. (1992). "Compressive strength of concrete at high temperatures: A reassessment." *Mag. Concrete Res.*, 44(161), 291–309.

Khoury, G. A., Grainger, B. N., and Sullivan, P. J. E. (1985). "Transient thermal strain of concrete: Literature review, conditions within specimen and behavior of individual constituents." *Mag. Concrete Res.*, 37(132), 131–144.

Kunieda, M., and Rokugo, K. (2006). "Recent progress on HPFRCC in Japan: Required performance and applications." *J. Adv. Concr. Technol.*, 4(1), 19–33.

Lam, L., Wong, Y. L., and Poon, C. S. (1998). "Effect of fly ash and silica fume on compressive and fracture behaviors of concrete." *Cement Concrete Res.*, 28(2), 271–280.

Lepech, M. D., and Li, V. C. (2008). "Large scale processing of engineered cementitious composites." *ACI Mater. J.*, 105(4), 358–366.

Li, V. C. (1998). "ECC-tailored composites through micromechanical modeling." *Proc., Int. Symp. on Fiber Reinforced Concrete: Present and the Future*, CSCE, Montreal, 64–97.

Li, V. C. (2003). "On engineered cementitious composites (ECC)–A review of the material and its applications." *Adv. Concrete Technol.*, 1(3), 215–230.

Li, V. C., Wang, S., and Wu, C. (2001). "Tensile strain-hardening behavior of PVA-ECC." *ACI Mater. J.*, 98(6), 483–492.

Mohamedbhai, G. T. G. (1986). "Effect of exposure time and rates of heating and cooling on residual strength of heated concrete." *Mag. Concrete Res.*, 38(136), 151–158.

Nasser, K. W., and Marzouk, H. M. (1979). "Properties of mass concrete containing fly ash at high temperatures." *ACI Mater. J.*, 76(4), 537–551.

Nishida, A., Yamazaki, N., Inoue, H., Schneider, U., and Diederichs, U. (1995). "Study on the properties of high strength concrete with short polypropylene fibers for spalling resistance." *Proc., Int. Symp. on*

Concrete Under Severe Environment, Vol. 2, K. Sakai, N. Banthia, and O. E. Gjorv, eds., 1141–1150.
Petzold, A., and Rohr, M. (1970). *Concrete for high temperatures*, McLaren and Sons, London.
Phan, L. T. (1996). "Fire performance of high strength concrete: A report of the state-of-the-art." U.S. Dept. of Commerce, Building and Fire Research Laboratory, NIST, Gaithersburg, MD.
Poon, C. S., Azhar, S., Anson, M., and Wong, Y. L. (2003). "Performance of metakaolin concrete at high temperatures." *Cement Concrete Res.*, 25(1), 83–9.
Poon, C. S., Lam, L., and Wong, Y. L. (1999). "Effects of fly ash and silica fume on interfacial porosity of concrete." *J. Mater. Civ. Eng.*, 11(3), 197–205.
Poon, C. S., Shui, Z. H., and Lam, L. (2004). "Compressive behavior of fiber reinforced high-performance concrete subjected to elevated temperatures." *Cement Concrete Res.*, 34(12), 2215–2222.
Rostasy, R. S., Weiss, R., and Wiedemann, G. (1980). "Changes of pore structure of cement mortar due to temperatures." *Cement Concrete Res.*, 10(2), 157–164.
Şahmaran, M., Lachemi, M., and Li, V. C. (2010). "Assessing the mechanical properties and microstructure of fire-damaged engineered cementitious composites." *ACI Mater. J.*, 107(3), 297–304.
Şahmaran, M., and Li, V. C. (2009). "Durability properties of micro-cracked ECC containing high volumes fly ash." *Cement Concrete Res.*, 39(11), 1033–1043.
Şahmaran, M., Yaman, I. O., and Tokyay, M. (2007). "Development of high volume low-lime and high-lime fly-ash-incorporated self consolidating concrete." *Mag. Concrete Res.*, 59(2), 97–106.
Sarvaranta, L., and Mikkola, E. (1994a). "Fibre mortar composites in fire conditions." *Fire Mater.*, 18(1), 45–50.
Sarvaranta, L., and Mikkola, E. (1994b). "Fibre mortar composites under fire conditions: Effects of ageing and moisture content of specimens." *Mater. Struct.*, 27(9), 532–538.
Taylor, H. F. W. (1964). *The chemistry of cements*, Academic Press, London.
Univ. of Michigan, ACE MRL. (2008). "Some ECC applications." ⟨http://ace-mrl.engin.umich.edu/NewFiles/eccapp.html⟩ (Oct. 11, 2010).
Wang, S., and Li, V. C. (2007). "Engineered cementitious composites with high-volume fly ash." *ACI Mater. J.*, 104(3), 233–241.
Wu, B., Su, X. P., Li, U., and Yuan, J. (2002). "Effect of high temperature on residual mechanical properties of confined and unconfined high strength concrete." *ACI Mater. J.*, 99(4), 399–407.
Xu, Y., Wong, Y. L., Poon, C. S., and Anson, M. (2001). "Impact of high temperature on PFA concrete." *Cement Concrete Res.*, 31(7), 1065–1073.
Xu, Y., Wong, Y. L., Poon, C. S., and Anson, M. (2003). "Influence of PFA on cracking of concrete and cement paste after exposure to high temperatures." *Cement Concrete Res.*, 33(12), 2009–2016.
Yang, E., Şahmaran, M., Yang, Y., and Li, V. C. (2009). "Rheological control in the production of engineered cementitious composites." *ACI Mater. J.*, 106(4), 357–366.
Yang, E. H., Yang, Y., and Li, V. C. (2007). "Use of high volumes of fly ash to improve ECC mechanical properties and material greenness." *ACI Mater. J.*, 104(6), 620–628.
Yigang, X., Wong, Y. L., Poon, C. S., and Anson, M. (2000). "Residual properties of PFA concrete subjected to high temperatures." *Proc., Int. Symp. on High Performance Concrete*.